Title

Fluorescent Guided Sentinel Lymph Mapping of the Oral Cavity with Fluorescent-Labeled Tilmanocept

Journal

The Laryngoscope, 134(3)

ISSN

0023-852X

Authors

Guo, Theresa

Jang, Sophie S

Ogawa, Ryotaro

et al.

Publication Date

2024-03-01

DOI

10.1002/lary.31014

Peer reviewed

HHS Public Access

Author manuscript

Laryngoscope. Author manuscript; available in PMC 2024 March 14.

Published in final edited form as:

Laryngoscope. 2024 March ; 134(3): 1299–1307. doi:10.1002/lary.31014.

Fluorescent guided Sentinel Lymph Mapping of the Oral Cavity with fluorescent-labeled tilmanocept

Theresa Guo, MD[1,2], **Sophie S. Jang, MD**[1,2], **Ryotaro Ogawa, MD**[2,3], **Morgan Davis, MD**[1,2], **Edward Ashworth, PhD**[2,3], **Christopher V. Barback, BS**[2,3], **David J. Hall, PhD**[2,3], **David R. Vera, PhD**[2,3]

[1]Department of Otolaryngology, Head and Neck Surgery, University of California, San Diego, La Jolla, CA

[2]Moores Cancer Center, University of California, San Diego, La Jolla, CA

[3]Department of Radiology, University of California, San Diego, La Jolla, CA

Abstract

Objective: With the shift toward utilization of sentinel lymph node biopsy (SLNB) in oral cavity cancer, improved techniques for intraoperative sentinel node identification are needed. This study investigates the feasibility of fluorescently labeled tilmanoscept in SLNB in an oral cancer rabbit model.

Methods: An animal study was designed using 21 healthy male New Zealand rabbits. Gallium-68-labeled tilmanocept labeled with IRDye800CW was injected submucosally into the buccal mucosa (n=6) or lateral tongue (n=7) followed by PET imaging. One hour after injection, SLNB was performed using fluorescence imaging followed by a bilateral neck dissection and sampling of non-nodal surrounding tissue. All tissues were measured for radioactivity and fluorescence. Additionally, eight rabbits were injected with delayed SLNB performed 48 hours after injection.

Results: Buccal injections all had ipsilateral SLN drainage and tongue injections exhibited 18.2% contralateral drainage. An average of 1.9±1.0 SLN (range 1–5) were identified. In addition, an average of 16.9±3.3 non-sentinel lymph nodes were removed per animal. SLNs had an average of 0.69±0.60 percent-of-injected dose (%ID) compared to non-sentinel nodes with 0.012±0.025 %ID and surrounding tissue with 0.0067±0.015 %ID. There was 98.0% agreement between sentinel lymph nodes identified using fluorescence compared to radioactivity with Cohen's kappa coefficient of 0.879. In 48-hour delayed SLNB, results were consistent with 97.8% agreement with radioactivity and Cohen's Kappa coefficient of 0.884. Fluorescence identified additional lymph nodes that were not identified by radioactivity, and with one false negative.

Corresponding Author: Theresa Guo, Assistant Professor, Surgery, Department of Otolaryngology, University of California, San Diego, 3855 Health Science Dr, MC 0987, La Jolla, CA 92093, twguo@health.ucsd.edu, Phone: +1 (858) 246-4541, Fax: +1 (858) 622-6198.

Conflicts of interest:
David Vera is the inventor of tilmanocept. All other authors have no conflicts of interest.

Conclusion: Fluorescent-labeled Tc-99m-tilmanocept represents a highly accurate adjunct to enhance SLNB for oral cavity cancer.

Level of Evidence: Preclinical study

Keywords

Oral cavity; sentinel lymph node biopsy; fluorescence guided surgery

Introduction

Sentinel lymph node biopsy (SLNB) is frequently performed in the head and neck region for treatment of melanoma, and emerging evidence now supports SLNB for early-stage oral cavity squamous cell carcinoma (OCSCC). In melanoma, the first Multicenter Selective Lymphadenectomy Trial (MSLT-1) established SLNB as standard of care for treatment of intermediate thickness melanoma.[1] Up to 20% of malignant melanoma occurs in the head and neck region.[2]

There is now a growing body of evidence that supports use of SLNB for treatment of early stage T1–2N0 OCSCC, including prospective trials, randomized controlled trials and meta-analyses.[3][Kang 36089746, Garrel, Hasegawa, Schilling London] In these patients, standard of care had previously been elective neck dissection, based on a randomized controlled trial showing significant improvement in survival with elective neck dissection compared with therapeutic neck dissection.[4] However, only about 20–30% of patients who undergo elective neck dissection will ultimately present with positive nodal disease.[4,5] Therefore, to reduce surgical morbidity recent studies have explored the role of SLNB for clinical N0 OCSCC. Two randomized clinical trials have now shown that SLNB can be performed in early stage OCSCC with similar recurrence free survival compared to elective neck dissection.[6,7] Currently, the NRG oncology group is enrolling patients in the United States for a similar randomized control trial to definitively establish the role of SLNB in this patient population.[8]

Within this context, there is a growing need for tools to support intraoperative sentinel lymph node (SLN) identification in the head and neck. Due to the dense network of lymph nodes in the head and neck, accurate and safe identification of SLNs can pose a unique challenge. SPECT/CT can provide anatomic correlation for improved identification of SLNs, especially in the parotid bed.[9–11] In addition, false negative rates are higher for floor of mouth lesions due to shine through effect, where the radiotracer signal from the primary site can obscure radioactivity in SLNs due to their close proximity.[3,12]

Current radiotracers such as technetium-99m (^{99m}Tc) labeled sulfur colloid, colloid albumin (Nanocoll)[13] or tilmanoscept (Lymphoseek)[14] provide spatial, but no intraoperative visual feedback. Isosulfan blue dye (Lymphazurin) is an adjunct to support sentinel lymph node identification, however is limited by quick passage of dye through the sentinel node.[15,16] Fluorescence guidance, specifically with Indocyanine green (ICG), has also been used to provide intraoperative visual feedback for sentinel node localization in both breast and oral cancer.[17,18] The utility of free ICG is also limited by only brief retention in

the sentinel node,[19] so ICG has been mixed with ^{99m}Tc-Nanocoll to allow non-covalent binding to the nanoparticle which promotes retention of both radioactivity and fluorescence within nodal tissue.[18] IRDye 800CW has also been tested with Nanocoll with strong fluorescence retention within SLNs.[20] Current consensus guidelines support use of optical tracers such ICG-^{99m}Tc-Nanocoll as adjuncts to improve localization of floor of mouth sentinel lymph nodes, by mitigating the shine through effect.[12,18] However adoption of ICG ^{99m}Tc-Nanocoll use is not universal. Nanocoll is not available in the United States, instead ^{99m}Tc labeled sulfur colloid and tilmanoscept (Lymphoseek) are primarily utilized for sentinel node biopsy, and fluorescent tracers combined with these agents could improve utilization in clinical practice. Lastly, surgeon experience plays a role in accurate SLNB, and additional tools to support clear identification of sentinel lymph nodes could improve learning curves.[21,22]

Recently, several studies have demonstrated the feasibility Tilmanoscept with covalently bound fluorescent label to provide visual feedback in addition to radiotracer signal as an adjunct for identification of sentinel lymph nodes in bladder, prostate and cervical cancer animal models.[23–25] Tc^{99m} Tilmanocept (Lymphoseek), which is distributed by Cardinal Health, has been widely adopted for SLNB since its FDA approval in 2013, and has been well studied in the head and neck.[26–29] This molecule features a low false negative rate due to its specificity to mannose receptors (CD206) expressed on the surface of macrophages and dendritic cells.[28–31] These studies demonstrated the accuracy of using fluorescence labeling for identification of SLNs, which was confirmed with radiolabeling. Therefore, we performed a feasibility study using the bimodal molecular imaging agent gallium-68-labeled IRDye800CW-tilmanocept, which carries both a radiolabel for gamma imaging and detection, and a fluorescent label. The purpose of this study is to determine the feasibility of fluorescence guided SLNB in an animal model of the oral cavity using this fluorescently labeled tilmanoscept.

Methods

Experimental design

We designed a non-survival study using twenty-one healthy male New Zealand white rabbits approved by the UCSD Institution Animal Care and Use Committee (S17047). All rabbits received injection in the buccal mucosa or oral tongue of dual labeled tilmanocept. After injection, the first set of 13 animals underwent positron-emission tomography (PET) imaging one hour after injection. SLN mapping and biopsy was then performed at either 1 hour (n=13) or 48 hours (n=8) following injection. SLNB was performed using fluorescence imaging camera *Fluobeam800* (Fluoptics, Grenoble, France). This was followed by a bilateral neck dissection including removal of submandibular and cervical nodes, sampling of non-nodal tissue adjacent to SLN(s), and resection of primary injection site. All tissues were measured individually for both radioactivity and fluorescence.

Molecular Imaging Agent Preparation and PET imaging

The fluorescent dye *IRDye800CW* (LI-COR Biosciences, Lincoln NE) was covalently attached[32] to tilmanocept (Navidea Biopharmaceuticals, Dublin OH) as shown in Figure

1. Radiolabeling[33] with Gallium-68 or Tc-99m were performed as previously described. Radiochemical and fluorescent purities were measured by instant thin layer chromatography, which exceeded 98%. The resulting bimodal molecular imaging agent is diagramed in Figure 1. Gallium-68 is a positron-emitting isotope with a 68-minute half-life, permitting imaging via PET and radioactivity measurement. The fluorescent tag, IRDye800, has an absorbance peak at 774 nm and a fluorescence peak at 789 nm.[34] This results in an imaging sensitivity with the *Fluobeam800* that is similar for IRDye800 and ICG.

Ga-68 labeled tilmanocept was injected (3 nmol, ~10MBq, 50ul) submucosally into four adjacent sites of the oral cavity (buccal mucosa or oral tongue, Figure 2a & 2b), mimicking peritumoral injection. Because SPECT imaging was not available for small animal experiments, PET imaging of the injection site and neck was obtained using a small animal PET imager (*eXplore Vista DR*; GE Healthcare; Waukesha, WI, Figure 2c), which has been previously validated for both Ga-68 and Tc-99 radiolabels.[33] PET imaging confirmed presence of sentinel node(s) after injection and laterality of SLNs. Additional imaging was performed distal to the injection site for a focused capture of the SLN(s). Images were reconstructed via ordered subset expectation maximization using a span of 3, Dmax of 16, 2 iterations and 16 subsets.

Tc-99m labeled tilmanocept (3nmol, ~74MBq, 50ul) was injected using the same protocol as Ga-68 labeled tilmanocept and was used for delayed experiments with SLNB performed at 48 hours after injection. After injection, rabbits were kept under free access to food and water as usual until time of SLNB dissection 48 hours after injection.

Fluorescence guided sentinel lymph node biopsy

The rabbit was euthanized by lethal injection of sodium pentobarbital at 150mg/kg prior to nodal dissection. Neck fur was shaved and removed for optimal visualization. The *Fluobeam800* near-fluorescent camera was used for fluorescence imaging, with exposure time of 500ms (Figure 2d). This exposure time was selected to allow for clear visualization of fluorescent signal through soft tissue, including prior to skin incision. Notably, gamma probes and radio-navigation were not use to localize sentinel nodes in this dissection. Once SLN was removed, fluorescence of the node was confirmed ex vivo. Four pieces of non-nodal tissue surrounding the SLN were then harvested. After the SLNB was complete including removal of any additional sentinel nodes, bilateral neck dissections were performed in the cervical and submandibular regions. Harvested SLN(s), non-sentinel lymph nodes, non-nodal tissue surrounding the SLN, and primary injection site were measured for weight, radioactivity, and fluorescence activity.

Radioactivity and fluorescence measurements

Radioactivity assays were performed on a gamma well counter *Wizard2* (PerkinElmer, Waltham, MA). All sample counts per minute were decay corrected and normalized using standards of the injected dose. Fluorescence images were taken with 10ms exposure time and evaluated via ImageJ. Brightness was calculated in arbitrary intensity units, with each unit corresponding to one of roughly 65K shades of gray.

Statistical analysis

Statistical analysis was performed with Prism 9 (GraphPad, San Diego, CA) software. Radioactivity and fluorescence levels were assessed by the unpaired Student's t-test. P values were 2-sided and differences were considered statistically significant at $p<0.05$. After identification of first echelon node, additional nodes were true considered sentinel nodes if radioactivity was measured at 10% or greater of radioactivity from first echelon sentinel node. Concordance between fluorescence identified SLN and those confirmed by radioactivity was calculated using Cohen's kappa coefficient.

Results

Sentinel lymph node distribution

An average of 1.9±1.0 SLN were identified across all rabbits using fluorescence guided imaging. Buccal injections resulted in more SLNs compared to tongue injections (2.5±1.1 vs. 1.3±0.5 SLN per animal, $p=0.003$). Buccal SLNs were all identified in the ipsilateral neck, while oral tongue SLNs were identified in the contralateral neck in two animals (18%, Table 1). Representative images from SLN evaluation are shown in Figure 3, highlighting the additional intraoperative visual feedback provided by the fluorescence imaging compared to white light (Video 1). From bilateral neck dissection, an average of 16.9±3.3 non-sentinel lymph nodes were removed per animal, including both the cervical and submandibular regions.

Radioactivity and fluorescence-based sentinel lymph node identification demonstrates high concordance

Fluorescence guided SLNB was performed and identified SLNs are summarized in Table 1. PET imaging preoperatively was used to guide SLN localization, including laterally and identification of multiple sentinel nodes. However, radiotracer probes were not used during SLNB, and SLNs were identified using fluorescence imaging alone during dissection. Furthermore, fluorescent SLNs were often visible prior to skin incision due to high penetrance. (Figure 3d & 3e).

Using these methods, 23 SLNs and 236 non-SLNs were identified with fluorescence guidance in 13 animals 1 hour after injection. First echelon SLN was identified in all animals. In 6 rabbits, only a single SLN was identified, and this was more common after oral tongue injection; of these one SLN was noted to be in the contralateral neck.

Fluorescence demonstrated high sensitivity for identification of sentinel nodes with four additional lymph nodes identified beyond what was considered positive by radioactivity, and one incidence of false negative. Additional lymph nodes were considered to be true sentinel nodes if radioactivity was ≥10% of first echelon SLN. Four SLNs were identified by fluorescence which were below the 10% threshold. These lymph nodes did demonstrate some radioactivity on ex vivo evaluation, but only 1.8–5.8% of first echelon node. Conversely, one sentinel lymph node with 16.6% radioactivity of first SLN was not detected during fluorescence guided dissection. On ex vivo analysis, this lymph node did exhibit some fluorescence (506 IU, compared to mean of 135.8 IU in other non-sentinel

lymph nodes). Notably, this additional lymph node was located in the cervical neck, while both SLNs identified during dissection were located in the submandibular region. Overall, there was 98.0% agreement between sentinel lymph nodes identified using fluorescence compared to radioactivity with Cohen's kappa coefficient of 0.879.

Radioactivity is specific to fluorescence identified sentinel lymph nodes

Radioactivity was measured in primary injection site, SLNs, non-SLNs and adjacent tissue. Radioactivity of primary injection site was 25.3±10.88% of injected dose (%ID). The radioactivity at the buccal injection site was 31.63±10.85% of injected dose (%ID) and 21.60±7.11% ID for the ipsilateral tongue injection sites. Tissue adjacent to the injection site had a mean of 0.85±0.92% ID. Radioactivity in first echelon nodes was 0.97±0.61% ID, representing 3.86% of radioactivity signal at the primary site.

Overall SLNs identified by fluorescence guided biopsy had significantly higher radioactivity signal compared to non-sentinel lymph nodes and surrounding tissue for both buccal and tongue injection sites (Figure 4). SLNs identified by fluorescence imaging demonstrated an average radioactivity of 0.69±0.60%ID compared to 0.012±0.025%ID in non-sentinel lymph nodes (representing 1.7% of SLN radioactivity) and surrounding tissue (0.0067±0.015%ID, representing 0.97% of SLN radioactivity). The surrounding tissue and non-sentinel nodes both demonstrated significantly decreased radioactivity compared to SLNs ($p<0.0001$).

Next, fluorescence was measured in each tissue by intensity unit (IU). Again, the injection site demonstrated the highest fluorescence intensity of 19,164.15±6,892.68 IU. There was minimal fluorescence in adjacent tissue at 186.39±82.57 IU (0.97% of primary site fluorescence). SLNs measured 2,509.49±2,581.45 IU (13.1% of primary site fluorescence). In comparison, tissue surrounding the SLN measured 171.15±136.60 (6.82% of SLN fluorescence) and non-SLN measured 151.28±97.37 (6.03% of SLN fluorescence). The surrounding tissue and non-sentinel nodes again demonstrated significantly decreased fluorescence intensity compared to SLNs ($p<0.0001$). In the oral tongue model, limited fluorescence measurements were taken demonstrating consistent results. SLNs measured 2,659.08±1,971.83 IU compared to surrounding tissue which measured 157.69±53.32 IU (similarly, 5.90% of SLN) and was significantly lower ($p<0.0001$).

48-hour Delayed sentinel lymph node biopsy

Using a modified protocol, eight additional animals received oral dual-labeled tilmanoscept injection (n=4 buccal, n=4 tongue) followed by a 48-hour delay before performing the SLNB to demonstrate the longevity of tracer signal. An average of 2.75±0.50 SLN were identified after buccal injection and 1.25±0.50 SLN following oral tongue injection. No significant difference was seen in the number of SLN identified in the immediate dissection and 48-hour delayed experimental designs (1.77±1.09 and 2.0±0.93, respectively; $p=0.63$)

Similar with the non-delayed dissection, the injection sites had the highest radioactivity (17.8±10.3%ID). Again, SLNs (1.23±1.05%ID) demonstrated significantly higher radioactivity compared to both non-sentinel lymph nodes (0.00097±0.001%ID, 0.08% of SLN signal, $p<0.001$) and surrounding tissue (0.0011±0.0014%ID, 0.09% of SLN signal, $p<0.001$).

With 48-hour delay, fluorescence was higher in SLNs compared to injection sites, likely due to accumulation of tracer over time. For buccal injections, injection site fluorescence was 3099.55±414.60 IU and 3580.12±1899.33 IU (116% of primary site signal) in SLNs. Similarly for tongue injection, SLN fluorescence was higher (4833.64±986.19 IU, 250% of primary site signal) than tongue injection sites (1931.96±1029.27 IU). Minimal fluorescence signal was seen in surrounding tissue (118.85±22.17 IU, 2.8% of SLN signal) and non-sentinel node tissue (114.11±20.27 IU, 2.7% of SLN signal).

During 48-hour delayed experiments, similar to immediate dissection some SLNs detected by fluorescence did not meet detection threshold based on radioactivity. Of 16 SLN visualized using intraoperative fluorescent imaging, three had <10% radioactivity of first echelon nodes. The measured fluorescence activity of these nodes was significantly decreased 1190±1226 IU compared to 4134±931 IU (p=0.008) of those confirmed by radioactivity. Therefore, decreased radioactivity correlated with decreased fluorescence signal, however these nodes were still identified as SLNs through visual feedback during sentinel node dissection. For delayed dissection, a total of 16 SLNs were identified by fluorescence and 119 non-sentinel nodes, resulting in 97.8% agreement with radioactivity and Cohen’s Kappa coefficient of 0.884.

Discussion

This study demonstrates the utility of an exciting emerging technology with fluorescent-labeled radiopharmaceutical tilmanocept for SLNB in the head and neck, specifically oral cavity. The fluorescent tracer demonstrated high concordance with radiotracer activity for both oral tongue and buccal injection sites. First echelon nodes were identified in all animals. The tracer demonstrated high specificity with surrounding tissue showing less than 1% radiotracer activity compared to sentinel nodes. There was clear delineation between SLNs compared to non-sentinel nodes, which only demonstrated 1.7% radioactivity and 6% fluorescence of sentinel node signal.

The tracer demonstrated 98% agreement between fluorescence identified SLNs and measured radioactivity. Main discordance was seen in greater sensitivity of the fluorescence signal resulting in additional SLNs being identified that were below the threshold to be considered SLNs by radioactivity. Use of this tracer as an adjunct to SLN could result in greater number of SLNs removed. Only one false negative was encountered using the fluorescence-based method, and this node was likely missed as it was located in a separate nodal basin than the first echelon sentinel node. This highlights the role for radioactivity probes and preoperative imaging, which were not used during these dissections, to assist in identification of additional sentinel nodes in separate nodal basins or contralateral. Notably, the false positive node did demonstrate fluorescence signal ex vivo, therefore no evidence of uncoupling of the fluorescence and radiotracer was observed, even after 48 hour delayed dissection.

Using novel dual-labeled tracers such as the proposed fluorescently labeled tilmanocept offers several advantages compared to other fluorescent imaging techniques such as indocyanine green alone.[17,18] With a dual-labeled tracer, injection of only one agent is

required to obtain both preoperative imaging and intraoperative visualization, in contrast to blue dye or free ICG. Hybrid ICG-^{99m}Tc-Nanocoll with non-covalent binding of ICG, which can be provided with a single injection, has been utilized in oral cancer to enhance identification of SLNs from oral cavity tumors.[18] However, lack of covalent bonding can result in potential uncoupling and flow through of ICG outside the true sentinel node(s), depending on purity of preparation (with removal of free ICG not bound to albumin colloid).[35] The proposed dual labeled tilmanoscept tracer offers the advantage of covalently bound fluorescence tag (Figure 1) which is extremely stable in vivo up to 72 hours.[33] Furthermore, with the specificity of tilmanocept to mannose receptors, this tracer can remain within the target SLNs for prolonged periods of time without flow through. In this study, our dual-labeled tilmanocept remained easily detectable in SLNs at 48 hours, consistent with studies in other anatomic sites.[24] The number of SLNs identified remained consistent between immediate SLN biopsy and after 48-hour delay, demonstrating the stability of this agent without evidence of uncoupling. Lastly, tilmanoscept (Lymphoseek from Cardinal Health) has had wide adoption in the United States since its FDA approval in 2013, and has been well validated for use in OSCC SLNB.[26–29]

We demonstrate feasibility of this technique for oral cavity injections—with both buccal and tongue injections demonstrating similar results. As strong evidence has arisen to support treatment of early-stage oral cavity squamous cell carcinoma with SLNB, tools to support safe performance of this surgery are needed. SLNB for oral cavity tumors poses unique challenges. Use of optical tracers has been recommended for sentinel lymph node biopsy of floor of mouth tumors,[12] however dual labeled agents are not currently available for use in the United States. Most oral cavity sites demonstrate an average of three SLNs.[6,7] Real time visual feedback from fluorescence could reduce surgery time for identification of multiple SLNs. The gamma probe provides the general region of SLNs, but the fluorescently tagged tracer can clarify localization of individual nodes, which is especially advantageous in a dense network of lymph nodes. In addition, in other regions of the head and neck fluorescence imaging could enhance parotid SLN identification within the parotid parenchyma and potentially decreasing extent of dissection to reduce risk for facial nerve injury. Lastly, floor of mouth lesions have been reported to have lower SLN identification, as radioactivity from the primary site can shine through to obscure SLN signal. Use of the fluorescently labeled radiotracer could overcome this shine through phenomenon which has been previously demonstrated with ICG-Tc^{99m} Nanocoll.[18]

This fluorescence system provides strong fluorescence signal which was even visible through the skin. The penetration depth of near infra-red fluorophores is general limited to 1–2 cm,[17] which was sufficient in the rabbit model to visualize sentinel nodes prior to skin incision, even for cervical nodes that reside deep to the neck musculature. However, in the clinical setting these penetration depths may not allow for immediate visualization of deep cervical nodes that lie under the sternocleidomastoid until after retraction. Other more superficial nodes such as parotid or external jugular nodes could be visualized transcutaneously in low BMI patients to assist in incision planning. In the study of 30 oral cavity patients using ICG-Tc^{99m} Nanocoll, 10% of SLNs were visible transcutaneously.[18] This may be especially useful in cases where SLNs reside in different nodal basins, requiring multiple incisions.

To translate these findings toward clinical use, future studies are also needed to confirm fluorescence visualization using existing intraoperative imaging tools. Prior studies have demonstrated feasibility using this dual labeled tracer using the FireFly system in conjunction with the DaVinci robotics system in other anatomic sites.[23,24] As robotic systems are not typically used for head and neck sentinel lymph node dissection, evaluation of other intraoperative imaging tools will be needed.

Conclusions

Evaluation of fluorescent-labeled tilmanocept demonstrates high feasibility and accuracy in oral cavity cancer and for identification of sentinel lymph nodes in a rabbit animal model. Use of intraoperative fluorescence imaging can enhance identification of sentinel lymph nodes. Future studies within clinical trials are needed to evaluate the potential surgical advantages of this fluorescent-labeled tilmanocept for head and neck sentinel lymph node biopsy.

Acknowledgements:

Disclosures:

Dr. David Vera is the inventor of tilmanoscept.

Funding:

This work was supported by 1KL2TR001444 from National Institutes of Health (Guo), Gleiberman Head & Neck Cancer Center, Early Career Faculty Award (Guo), and the American Cancer Society IRG Grant # IRG-19-230-48-IRG (Guo) and UC San Diego Moores Cancer Center, Specialized Cancer Center Support Grant NIH/NCI P30CA023100 (Guo).

References

1. Morton DL, Thompson JF, Cochran AJ, et al. Final trial report of sentinel-node biopsy versus nodal observation in melanoma. N Engl J Med. Feb 13 2014;370(7):599–609. doi:10.1056/NEJMoa1310460 [PubMed: 24521106]
2. Larson DL, Larson JD. Head and neck melanoma. Clin Plast Surg. Jan 2010;37(1):73–7. doi:10.1016/j.cps.2009.08.005 [PubMed: 19914460]
3. Schilling C, Stoeckli SJ, Haerle SK, et al. Sentinel European Node Trial (SENT): 3-year results of sentinel node biopsy in oral cancer. Eur J Cancer. Dec 2015;51(18):2777–84. doi:10.1016/j.ejca.2015.08.023 [PubMed: 26597442]
4. D'Cruz AK, Vaish R, Kapre N, et al. Elective versus Therapeutic Neck Dissection in Node-Negative Oral Cancer. N Engl J Med. Aug 6 2015;373(6):521–9. doi:10.1056/NEJMoa1506007 [PubMed: 26027881]
5. de Bree R, Takes RP, Shah JP, et al. Elective neck dissection in oral squamous cell carcinoma: Past, present and future. Oral Oncol. Mar 2019;90:87–93. doi:10.1016/j.oraloncology.2019.01.016 [PubMed: 30846183]
6. Garrel R, Poissonnet G, Moyà Plana A, et al. Equivalence Randomized Trial to Compare Treatment on the Basis of Sentinel Node Biopsy Versus Neck Node Dissection in Operable T1-T2N0 Oral and Oropharyngeal Cancer. J Clin Oncol. Dec 1 2020;38(34):4010–4018. doi:10.1200/jco.20.01661 [PubMed: 33052754]
7. Hasegawa Y, Tsukahara K, Yoshimoto S, et al. Neck Dissections Based on Sentinel Lymph Node Navigation Versus Elective Neck Dissections in Early Oral Cancers: A Randomized, Multicenter, and Noninferiority Trial. J Clin Oncol. Jun 20 2021;39(18):2025–2036. doi:10.1200/jco.20.03637 [PubMed: 33877855]

8. Lai SY. Comparing Sentinel Lymph Node (SLN) Biopsy With Standard Neck Dissection for Patients With Early-Stage Oral Cavity Cancer. In: Oncology N, editor.: https://ClinicalTrials.gov/show/NCT04333537.
9. Sethi RKV, Abt NB, Remenschneider A, Wang Y, Emerick KS. Value of SPECT/CT for Sentinel Lymph Node Localization in the Parotid and External Jugular Chain. Otolaryngol Head Neck Surg. Nov 2018;159(5):866–870. doi:10.1177/0194599818786946 [PubMed: 29986639]
10. Noorbakhsh S, Papageorge M, Maina RM, et al. Methods of Sentinel Lymph Node Identification in Auricular Melanoma. Plast Reconstr Surg Glob Open. Dec 2021;9(12):e4004. doi:10.1097/gox.0000000000004004 [PubMed: 34938645]
11. Zender C, Guo T, Weng C, Faulhaber P, Rezaee R. Utility of SPECT/CT for periparotid sentinel lymph node mapping in the surgical management of head and neck melanoma. Am J Otolaryngol. Jan-Feb 2014;35(1):12–8. doi:10.1016/j.amjoto.2013.08.004 [PubMed: 24140088]
12. Schilling C, Stoeckli SJ, Vigili MG, et al. Surgical consensus guidelines on sentinel node biopsy (SNB) in patients with oral cancer. Head Neck. Aug 2019;41(8):2655–2664. doi:10.1002/hed.25739 [PubMed: 30896058]
13. Gommans GM, Gommans E, van der Zant FM, Teule GJ, van der Schors TG, de Waard JW. 99mTc Nanocoll: a radiopharmaceutical for sentinel node localisation in breast cancer--in vitro and in vivo results. Appl Radiat Isot. Sep 2009;67(9):1550–8. doi:10.1016/j.apradiso.2009.02.091 [PubMed: 19328701]
14. Wallace AM, Hoh CK, Ellner SJ, Darrah DD, Schulteis G, Vera DR. Lymphoseek: a molecular imaging agent for melanoma sentinel lymph node mapping. Ann Surg Oncol. Feb 2007;14(2):913–21. doi:10.1245/s10434-006-9099-4 [PubMed: 17146742]
15. Montgomery LL, Thorne AC, Van Zee KJ, et al. Isosulfan blue dye reactions during sentinel lymph node mapping for breast cancer. Anesth Analg. Aug 2002;95(2):385–8, table of contents. doi:10.1097/00000539-200208000-00026 [PubMed: 12145056]
16. Echt ML, Finan MA, Hoffman MS, Kline RC, Roberts WS, Fiorica JV. Detection of sentinel lymph nodes with lymphazurin in cervical, uterine, and vulvar malignancies. South Med J. 1999/02// 1999;92(2):204–208. doi:10.1097/00007611-199902000-00008
17. Kitai T, Kawashima M. Transcutaneous detection and direct approach to the sentinel node using axillary compression technique in ICG fluorescence-navigated sentinel node biopsy for breast cancer. Breast Cancer. Oct 2012;19(4):343–8. doi:10.1007/s12282-011-0286-1 [PubMed: 21725656]
18. Christensen A, Juhl K, Charabi B, et al. Feasibility of Real-Time Near-Infrared Fluorescence Tracer Imaging in Sentinel Node Biopsy for Oral Cavity Cancer Patients. Ann Surg Oncol. Feb 2016;23(2):565–72. doi:10.1245/s10434-015-4883-7 [PubMed: 26467454]
19. Stoffels I, Dissemond J, Poppel T, Schadendorf D, Klode J. Intraoperative Fluorescence Imaging for Sentinel Lymph Node Detection: Prospective Clinical Trial to Compare the Usefulness of Indocyanine Green vs Technetium Tc 99m for Identification of Sentinel Lymph Nodes. JAMA Surg. Jul 2015;150(7):617–23. doi:10.1001/jamasurg.2014.3502 [PubMed: 26017057]
20. Heuveling DA, Visser GW, de Groot M, et al. Nanocolloidal albumin-IRDye 800CW: a near-infrared fluorescent tracer with optimal retention in the sentinel lymph node. Eur J Nucl Med Mol Imaging. Jul 2012;39(7):1161–8. doi:10.1007/s00259-012-2080-5 [PubMed: 22349719]
21. Orr RK, Hoehn JL, Col NF. The learning curve for sentinel node biopsy in breast cancer: practical considerations. Arch Surg. Jul 1999;134(7):764–7. doi:10.1001/archsurg.134.7.764 [PubMed: 10401830]
22. Ross GL, Shoaib T, Scott J, Soutar DS, Gray HW, MacKie R. The learning curve for sentinel node biopsy in malignant melanoma. Br J Plast Surg. Jun 2002;55(4):298–301. doi:10.1054/bjps.2002.3825 [PubMed: 12160535]
23. Liss MA, Stroup SP, Qin Z, et al. Robotic-assisted Fluorescence Sentinel Lymph Node Mapping Using Multimodal Image Guidance in an Animal Model. Urology. 2014/10/01/2014;84(4):982.e9–982.e14. doi:10.1016/j.urology.2014.06.021
24. Anderson KM, Barback CV, Qin Z, et al. Molecular Imaging of endometrial sentinel lymph nodes utilizing fluorescent-labeled Tilmanocept during robotic-assisted surgery in a porcine model. PLoS One. 2018;13(7):e0197842. doi:10.1371/journal.pone.0197842 [PubMed: 29965996]

25. Lee HJ, Barback CV, Hoh CK, et al. Fluorescence-Based Molecular Imaging of Porcine Urinary Bladder Sentinel Lymph Nodes. J Nucl Med. Apr 2017;58(4):547–553. doi:10.2967/jnumed.116.178582 [PubMed: 28153955]
26. Leong SP. Detection of melanoma, breast cancer and head and neck squamous cell cancer sentinel lymph nodes by Tc-99m Tilmanocept (Lymphoseek®). Clin Exp Metastasis. Dec 28 2021;doi:10.1007/s10585-021-10137-4
27. Kågedal Å, Margolin G, Held C, et al. A Novel Sentinel Lymph Node Approach in Oral Squamous Cell Carcinoma. Curr Pharm Des. 2020;26(31):3834–3839. doi:10.2174/1381612826666200213100750 [PubMed: 32053068]
28. Agrawal A, Civantos FJ, Brumund KT, et al. [(99m)Tc]Tilmanocept Accurately Detects Sentinel Lymph Nodes and Predicts Node Pathology Status in Patients with Oral Squamous Cell Carcinoma of the Head and Neck: Results of a Phase III Multi-institutional Trial. Ann Surg Oncol. Oct 2015;22(11):3708–15. doi:10.1245/s10434-015-4382-x [PubMed: 25670018]
29. Marcinow AM, Hall N, Byrum E, Teknos TN, Old MO, Agrawal A. Use of a novel receptor-targeted (CD206) radiotracer, 99mTc-tilmanocept, and SPECT/CT for sentinel lymph node detection in oral cavity squamous cell carcinoma: initial institutional report in an ongoing phase 3 study. JAMA Otolaryngol Head Neck Surg. Sep 2013;139(9):895–902. doi:10.1001/jamaoto.2013.4239 [PubMed: 24051744]
30. Wallace AM, Han LK, Povoski SP, et al. Comparative evaluation of [(99m)tc]tilmanocept for sentinel lymph node mapping in breast cancer patients: results of two phase 3 trials. Ann Surg Oncol. Aug 2013;20(8):2590–9. doi:10.1245/s10434-013-2887-8 [PubMed: 23504141]
31. Vera DR, Wallace AM, Hoh CK, Mattrey RF. A synthetic macromolecule for sentinel node detection: (99m)Tc-DTPA-mannosyl-dextran. J Nucl Med. Jun 2001;42(6):951–9. [PubMed: 11390562]
32. Zhengtao Q, David JH, Michael AL, et al. Optimization via specific fluorescence brightness of a receptor-targeted probe for optical imaging and positron emission tomography of sentinel lymph nodes. Journal of Biomedical Optics. 8/1 2013;18(10):1–13. doi:10.1117/1.JBO.18.10.101315
33. Qin Z, Hoh CK, Hall DJ, Vera DR. A tri-modal molecular imaging agent for sentinel lymph node mapping. Nuclear Medicine and Biology. 2015/12/01/ 2015;42(12):917–922. doi:10.1016/j.nucmedbio.2015.07.011
34. Qin Z, Hall DJ, Liss MA, et al. Optimization via specific fluorescence brightness of a receptor-targeted probe for optical imaging and positron emission tomography of sentinel lymph nodes. J Biomed Opt. Oct 2013;18(10):101315. doi:10.1117/1.JBO.18.10.101315 [PubMed: 23958947]
35. Buckle T, van Leeuwen AC, Chin PT, et al. A self-assembled multimodal complex for combined pre- and intraoperative imaging of the sentinel lymph node. Nanotechnology. Sep 3 2010;21(35):355101. doi:10.1088/0957-4484/21/35/355101 [PubMed: 20689167]

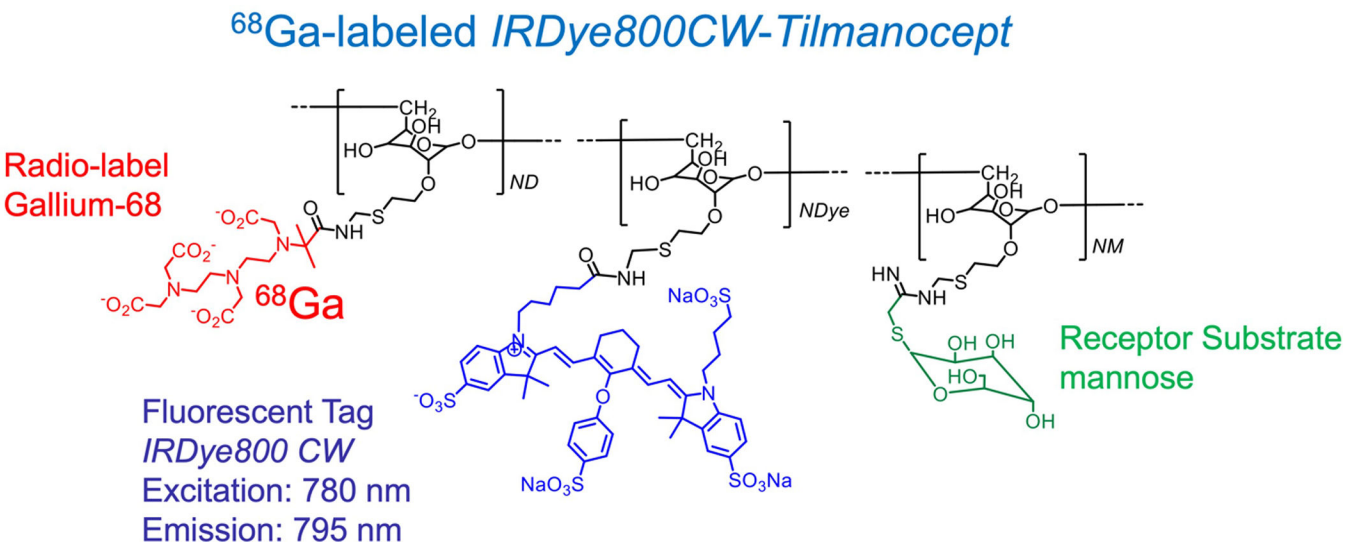

Figure 1.

The bimodal molecular imaging agent[^{68}Ga]*IRDye800*-tilmanocept consists of a near infrared fluorophore, IRDye800CW and the radiolabel gallium-68. An average of 25 mannose units are attached to the dextran backbone to provide high affinity for the receptor CD206.

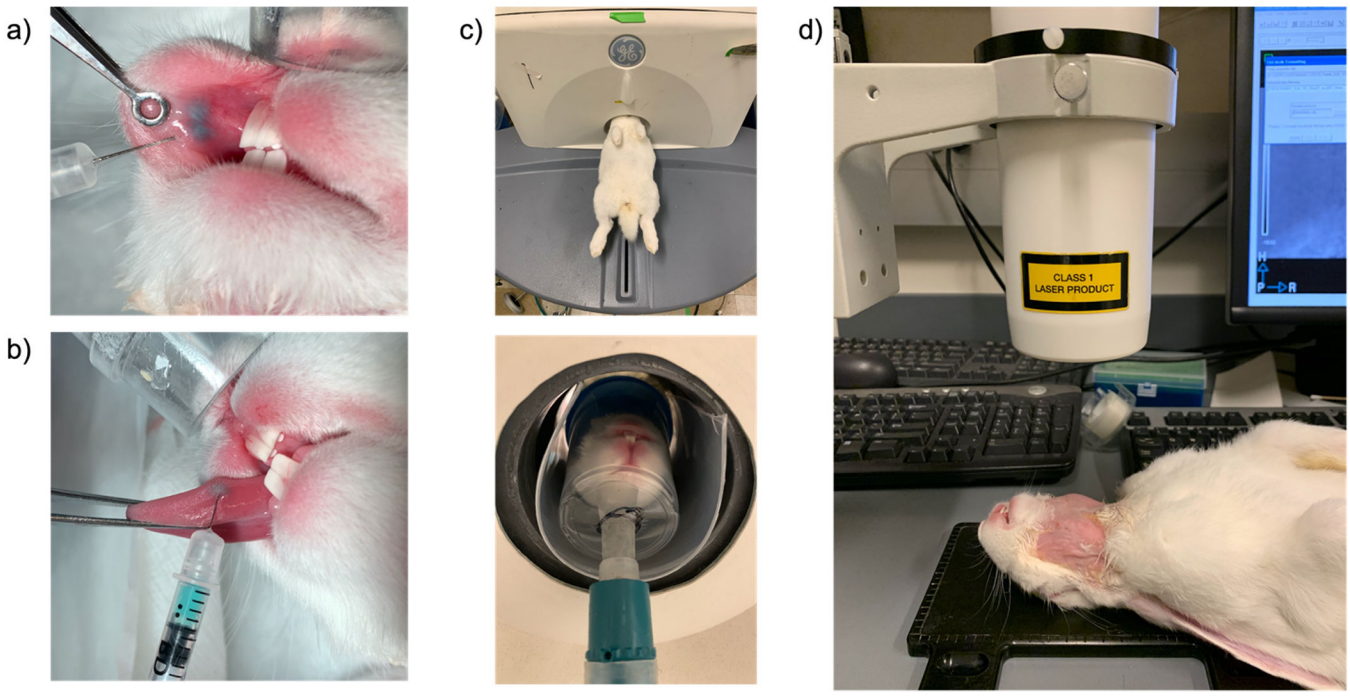

Figure 2.

Experimental set up demonstrating (a) buccal mucosa and (b) oral tongue injection with dual labeled tracer, (c) PET imaging set up and (d) fluorescence dissection set up with *Fluobeam800* camera

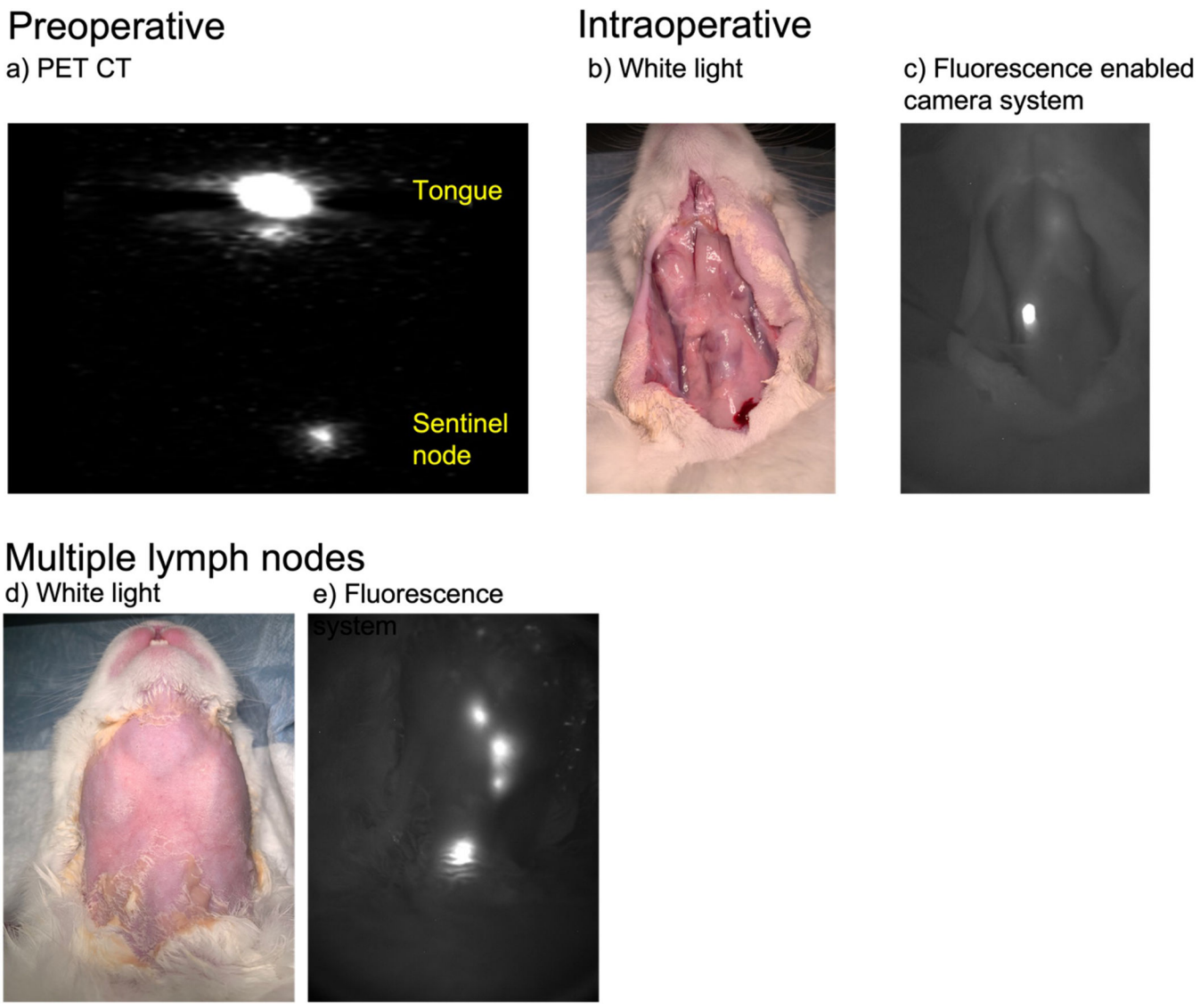

Figure 3.

Imaging modalities used in the study (a) preoperative injection PET imaging demonstrating sentinel node (b) intraoperative white light (c) intraoperative fluorescent enabled camera system at 500ms exposure time. (d & e) Multiple SLNs were visible using through the skin using fluorescence enabled camera system

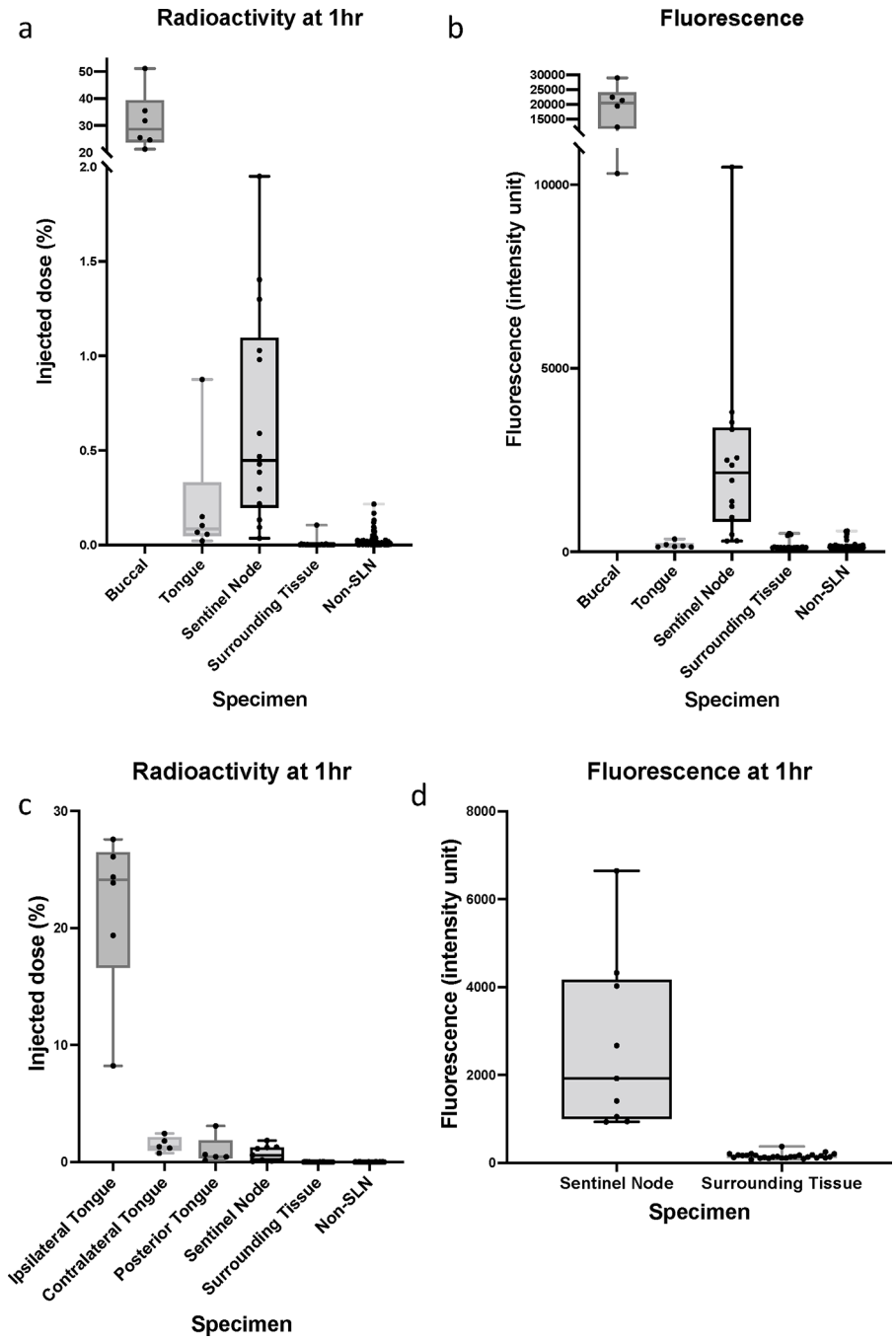

Figure 4.

Radioactivity and Fluorescence measurements: (a) Buccal injection - Detected radioactivity measured as percentage of injected dose (ID%) in buccal mucosa (b) Buccal injection - Detected fluorescence measured by relative intensity unit (c) Oral tongue-Detected radioactivity measured as percent injected dose to oral tongue (d) Oral tongue-Detected fluorescence measured by relative intensity unit in sentinel and non-sentinel node tissue

Video 1.

Identification and removal of sentinel lymph node. Side by side view in white light and with fluorescence enabled camera system

Table 1.

SLN characterization comparing SLN identified by fluorescence compared to radioactivity

Animal	SLN laterality	#SLN by fluoro	# SLN by radio	% radioactivity of additional SLNs compared to first echelon node*	
Buccal-1	Ipsilateral	5	3	1.8–24%	Five SLN identified, two showing 19.7% and 24% of SLN radioactivity, additional two below threshold for radioactivity detection (1.8–4.8%)
Buccal-2	Ipsilateral	2	2	60.20%	Two sentinel nodes identified, consistent with radioactivity
Buccal-3	Ipsilateral	1	1	-	
Buccal-4	Ipsilateral	2	2	28.80%	Two sentinel nodes identified, consistent with radioactivity
Buccal-5	Ipsilateral	2	3	10.2–16.6%	Two SLN identified on fluorescence; an additional lymph node demonstrated 16.6% radioactivity signal compared to first echelon LN but was not identified in fluorescence dissection
Buccal-6	Ipsilateral	2	2	51%	Two sentinel nodes identified, consistent with radioactivity
Tongue-7	Ipsilateral	1	1	-	
Tongue-8	Ipsilateral	2	1	5.30%	Two SLNs identified on fluorescence imaging, second node below threshold for radioactivity detection
Tongue-9	Contralateral	1	1	-	Single contralateral SLN identified
Tongue-10	Ipsilateral	1	1	-	
Tongue-11	Ipsilateral	1	1	-	
Tongue-12	Ipsilateral	2	1	5.80%	Two SLNs identified on fluorescence imaging, second node below threshold for radioactivity detection
Tongue-13	Ipsilateral	1	1	-	
48 hour delayed dissections					
Buccal-14	Ipsilateral	2	1	0.50%	Two SLNs identified on fluorescence imaging, second node below threshold for radioactivity detection
Buccal-15	Ipsilateral	3	3	12–30%	Three sentinel nodes identified, consistent with radioactivity
Buccal-16	Ipsilateral	3	3	23.7–47.3%	Three sentinel nodes identified, consistent with radioactivity
Buccal-17	Ipsilateral	3	1	3.6–5.4%	Three SLNs identified on fluorescence imaging, additional nodes below threshold for radioactivity detection
Tongue-18	Ipsilateral	1	1	-	
Tongue-19	Ipsilateral	1	1	-	
Tomgue-20	Bilateral	2	2	40.30%	Two sentinel nodes identified, second node in contralateral neck
Tongue-21	Ipsilateral	1	1	-	

* Lymph node considered true sentinel node by radioactivity if ≥10% radioactivity compared to first echelon sentinel node